World Journal of
Orthopedics

WJO *World Journal of* *Orthopedics*

Contents

Contents

SYSTEMATIC REVIEWS

Contents

ABOUT COVER

Editorial Board Member of *World Journal of Orthopedics*, Stuart Adam Callary, BSc, PhD, Postdoctoral Fellow, Research Scientist, Senior Lecturer, Department of Orthopaedics and Trauma, Royal Adelaide Hospital, Adelaide 5000, Australia. stuart.callary@sa.gov.au

AIMS AND SCOPE

The primary aim of *World Journal of Orthopedics* (*WJO*, *World J Orthop*) is to provide scholars and readers from various fields of orthopedics with a platform to publish high-quality basic and clinical research articles and communicate their research findings online.

  WJO mainly publishes articles reporting research results and findings obtained in the field of orthopedics and covering a wide range of topics including arthroscopy, bone trauma, bone tumors, hand and foot surgery, joint surgery, orthopedic trauma, osteoarthropathy, osteoporosis, pediatric orthopedics, spinal diseases, spine surgery, and sports medicine.

INDEXING/ABSTRACTING

The *WJO* is now abstracted and indexed in PubMed, PubMed Central, Emerging Sources Citation Index (Web of Science), Scopus, China National Knowledge Infrastructure (CNKI), China Science and Technology Journal Database (CSTJ), and Superstar Journals Database. The 2021 edition of Journal Citation Reports® cites the 2020 Journal Citation Indicator (JCI) for *WJO* as 0.66. The *WJO*'s CiteScore for 2020 is 3.2 and Scopus CiteScore rank 2020: Orthopedics and Sports Medicine is 87/262.

RESPONSIBLE EDITORS FOR THIS ISSUE

ORIGINAL ARTICLE

Observational Study

High-resolution, three-dimensional magnetic resonance imaging axial load dynamic study improves diagnostics of the lumbar spine in clinical practice

Tomasz Lorenc, Marek Gołębiowski, Wojciech Michalski, Wojciech Glinkowski

ORCID number: Tomasz Lorenc 0000-0002-9780-9484; Marek Gołębiowski 0000-0003-0721-1663; Wojciech Michalski 0000-0003-4366-6104; Wojciech Glinkowski 0000-0003-2602-1128.

Author contributions: Lorenc T, Gołębiowski M and Michalski W designed the research and collected the data; Lorenc T and Michalski W analyzed the data; Lorenc T and Gołębiowski M wrote the paper; Lorenc T and Glinkowski W contributed to manuscript revision; all authors approved the final version of the manuscript.

Institutional review board statement: The study was conducted according to the guidelines of the Declaration of Helsinki and approved by the Institutional Bioethical Review Board at Medical University of Warsaw (AKBE/100/13—obtained on December 10, 2013).

Informed consent statement: Informed consent was obtained from all subjects involved in the study.

Conflict-of-interest statement: The authors declare that there is no conflict of interest.

Tomasz Lorenc, Marek Gołębiowski, I[st] Department of Clinical Radiology, Medical University of Warsaw, Warsaw 02-004, Poland

Wojciech Michalski, Department of Mathematical Oncology, Maria Skłodowska-Curie National Research Institute of Oncology, Warsaw 02-781, Poland

Wojciech Glinkowski, Center of Excellence "TeleOrto" for Telediagnostics and Treatment of Disorders and Injuries of the Locomotor System, Department of Medical Informatics and Telemedicine, Medical University of Warsaw, Warsaw 00-581, Poland

Corresponding author: Tomasz Lorenc, MD, PhD, Associate Professor, I[st] Department of Clinical Radiology, Medical University of Warsaw, 5 Chalubinskiego Street, Warsaw 02-004, Poland. tlorenc@wum.edu.pl

Abstract

BACKGROUND
The response to axial physiological pressure due to load transfer to the lumbar spine structures is among the various back pain mechanisms. Understanding the spine adaptation to cumulative compressive forces can influence the choice of personalized treatment strategies.

AIM
To analyze the impact of axial load on the spinal canal's size, intervertebral foramina, ligamenta flava and lumbosacral alignment.

METHODS
We assessed 90 patients using three-dimensional isotropic magnetic resonance imaging acquisition in a supine position with or without applying an axial compression load. Anatomical structures were measured in the lumbosacral region from L1 to S1 in lying and axially-loaded magnetic resonance images. A paired *t* test at $\alpha = 0.05$ was used to calculate the observed differences.

RESULTS
After axial loading, the dural sac area decreased significantly, by 5.2% on average (4.1%, 6.2%, $P < 0.001$). The intervertebral foramina decreased by 3.4% (2.7%, 4.1%, $P < 0.001$), except for L5-S1. Ligamenta flava increased by 3.8% (2.5%, 5.2%,

P < 0.001), and the lumbosacral angle increased.

CONCLUSION
Axial load exacerbates the narrowing of the spinal canal and intervertebral foramina from L1-L2 to L4-L5. Cumulative compressive forces thicken ligamenta flava and exaggerate lumbar lordosis.

Key Words: Lumbar spine; Low back pain; Musculoskeletal disorder; Diagnosis; Axial loading; Magnetic resonance imaging; Spine biomechanics

Core Tip: In this study, a statistically proven correlation was made between the axial loading and lumbar spinal stenosis, thickening of the ligamenta flava, narrowing of the intervertebral foramina from L1-L2 to L4-L5 and lumbar lordosis exaggeration. A novel aspect of this study was a simultaneous comparison of the dural sac size, ligamenta flava thickness, foraminal dimensions and lumbar sagittal alignment between axial loaded and recumbent three-dimensional high-resolution magnetic resonance imaging in an extensive group of lower back pain patients. This was done to conduct a detailed evaluation for better spinal surgery decision-making and spinal injections.

INTRODUCTION

Lower back pain (LBP) remains a major worldwide public health problem that has increased substantially over several decades[1]. The problem of LBP affects epidemiology[2-5], health economics[6,7] and social aspects (disability, inability to work, limited daily activity)[8]. LBP is a common problem affecting most adults at some point during their lifetime[3,4,9]. More than half of the population may experience a pain relapse within a year, and 8% of people will have chronic pain[10]. In their systematic review, Meucci *et al*[11] revealed that chronic LBP prevalence was 4.2% in individuals aged between 24 and 39 years. The LBP prevalence equals 19.6% between 20 and 59 years of age and increases linearly from the third decade of life until 60. Chronic LBP is a significant contributor to the global disability burden[12]. Disability besides pain due to LBP is reported frequently and continues to be the leading cause of years lived with disability[13].

The vertically-oriented human spine acts as a dynamic and static column connecting the skeletal system. Substantial forces act on the longitudinal axis of the spine in the human's upright position. Spinal compression is traditionally considered the primary biomechanical mechanism associated with work-related LBP[14,15]. Human erect position can lead to increased axial compression in the lumbar spine and several side effects, including back pain. The lifting of objects raises the axial compression in the lumbar spine and increases LBP risk[16-19].

The classic works of Nachemson *et al*[20,21] from the early 1960s showed that the highest degree of intradiscal pressure in the lumbar spine occurs in standing and sitting positions, mainly when a person leans forward. The intradiscal pressure is lower when an individual is in the lying position than in the sitting and standing positions[22]. These observations were confirmed by Rohlmann *et al*[23,24] using wireless measurement. Schonstrom *et al*[25] showed that the intradiscal force difference measured at rest and axial loading acting on the spine reaches 500 N on human spine segments. The difference in intradiscal pressure observed in the spine segments is comparable to the values found in volunteers subjected to different loads and different body positions[21].

Correct, quick and precise determination of the underlying causes of back pain symptoms is crucial for many patients. Imaging for LBP is considered appropriate when clinical suspicion of severe pathology or surgery addresses a specific pathology [26,27]. Imaging may also be used to diagnose chronic LBP; however, particular indicators for appropriate imaging use are less well defined, with pain lasting longer than 6 weeks being an indicator for imaging in some guidelines but not in others[26]. Axial compression imaging may improve the diagnostics in clinical management of LBP and improve appropriate treatment decisions[28-30].

Even though the highest spinal loading occurs in the upright and sitting positions, a typical magnetic resonance imaging (MRI) examination is performed with the patient lying supine when no loads are exerted on the spine. As a result, the lying position of the examined patient poses a limitation on magnetic resonance tomography. An attempt at overcoming MRI limitations caused by the patient being in a lying position led to the introduction in clinical practice of an examination performed in the supine position with axial loading, simulating physiological loading. The load distribution among lumbar spinal structures, in general, is still an unanswered question and should be the focus of biomechanical testing. Previous studies showed that axial-loaded MRI could simulate the standing position and reveal additional valuable pathological findings not detected by conventional recumbent MRI[31,32]. Compressive loads on the vertebral discs are not the only ones occurring in the spine; load indicators other than disc compression are at least equally relevant, so attention should be paid to them. Few studies simultaneously investigated several anatomical structures in the lumbar spine using upright, open and low-field MRI[33] or axial loaded MRI[16]. However, these studies did not use dynamic three-dimensional (3D) high-resolution images and failed to measure the ligamentum flavum area, foraminal area and lumbar lordosis.

Moreover, previous studies were performed in a young, small group of asymptomatic volunteers[33], or simultaneous measurements were not correlated between the sets of variables[16]. No study has simultaneously compared dural sac size, ligamenta flava thickness, foraminal dimensions and lumbar sagittal alignment between axial-loaded and recumbent MRI in a large group of LBP patients to identify dynamic changes and associations between morphology and demography. Therefore, this study's objective was to evaluate and measure the changes presented by MRI of selected lumbar spine structures upon axial-loading compared with recumbent MRI and correlate them to morphologic changes and demographic data. Additionally, the study aimed to assess the value and potential use of axial loading in lumbar spine examinations. The detailed evaluation seems crucial for spinal surgery decision-making. The spinal injections or transforaminal[34,35] or interlaminar spinal endoscopy[36,37] can be used to relieve symptoms due to the intervertebral foramen narrowing or spinal canal stenosis caused by the thickening of the ligamentum flavum.

MATERIALS AND METHODS

We enrolled 90 patients diagnosed at the Magnetic Resonance Laboratory with LBP inclusion criteria as an indication. Exclusion criteria included significant spinal injury, osteoporosis, previous spine surgery, lack of good patient cooperation, a body mass below 40 kg and a lack of written consent from the patient. General contraindications for MRI examinations (*e.g.*, pacemakers, ferromagnetic implants, foreign bodies and claustrophobia) were also considered. A total of 46 (51%) men and 44 (49%) women were included in the study with an age and body mass index (mean ± standard deviation) of 49 ± 16 years and 26.0 ± 4.2 kg/m^2, respectively. The study was conducted according to the Declaration of Helsinki guidelines and approved by the Institutional Bioethical Review Board at Medical University of Warsaw (AK-BE/100/13 — obtained on December 10, 2013). Informed consent was obtained from all subjects involved in the study.

Lumbar spine MRI examination protocol without and after axial loading

The examination was performed using a 1.5 T MRI (Ingenia; Philips Healthcare, Eindhoven, The Netherlands). After performing recumbent MRI examinations, axial loading was applied using an external commercially available nonmagnetic DynaWell (DynaWell L-Spine; DynaWell Diagnostics, Las Vegas, NV, United States) compression device. The phase without axial loading was identical to a standard lumbar spine examination. Both the axial-loaded and unloaded MRI examinations were performed with a 3D T2-weighted Volume ISotropic Turbo spin-echo

Acquisition sequence (Table 1). According to previous disc pressure measurements[21] the chosen load was equal to 40%-50% of the patient's body weight, with equal load distribution on both legs (20%-25% of patient body mass per leg). The patient was subjected to this load in the lying position for at least 5 min before the examination.

Image analysis

Images were assessed on a dedicated workstation (IntelliSpace Portal; Philips Healthcare, Eindhoven, The Netherlands) at a single center. Based on recumbent and axial-loaded MRIs, the lumbosacral angles between the superior vertebral endplate of L1 and superior vertebral endplate of S1 were measured, enabling the observation of spine adaptations at a whole lumbar level (Figure 1). The dural sac cross-sectional area was calculated for each level from L1-L2 to L5-S1 for examination with and without axial loading. Measurements were performed by encircling the dural sac transverse area, capturing T2-weighted MRI at the same levels for phases without and with axial loading with the plane precisely positioned parallel to the midplane of the intervertebral disc (Figure 1). The vertebral foramina sagittal cross-section area was determined for each level, from L1-L2 to L5-S1, on both sides. Measurements were performed by encircling the vertebral foramina area in sagittal cross-sections on the same levels for the phase with and without axial loading (Figure 1). The cross-sectional area of the ligamentum flavum was determined for levels from L1-L2 to L5-S1 on both sides. The measurements were captured by encircling the area of the ligamentum flavum in cross-sections at facet joint levels with and without axial loading (Figure 1). The degree of disc and facet joint degeneration, the degree of spinal canal stenosis, the degree of foraminal stenosis and the degree of disc herniation were assessed on recumbent images on all disc levels according to the classifications of Pfirrmann *et al* [38], Weishaupt *et al*[39], Schizas *et al*[40], Lee *et al*[41] and the Michigan State University classification of lumbar disc herniation[42].

Statistical analysis

The assessment criterion used was the percentage difference of measured parameters with a 95% confidence interval (CI). A paired *t* test was applied at an α = 0.05 level to verify the hypothesis regarding the statistical significance of changes observed. The Pearson correlation test was used to explore the mutual relations of the spine structural parameters. A paired *t* test was applied to determine the relationship between age and sex for each measured parameter. The statistical methods of this study were reviewed by Wojciech Michalski from the Department of Mathematical Oncology, Maria Skłodowska-Curie National Research Institute of Oncology, Warsaw, Poland. The IBM SPSS Statistics (IBM Corp., Armonk, NY, United States) version 20 for Linux OS was used for statistical analysis.

RESULTS

Ligamentum flavum

Upon axial loading, the area of the ligamenta flava was statistically significantly increased on average by 3.8% (95%CI: 2.5%, 5.2%, *P* < 0.001; Table 2).

Dural sac

Upon axial loading, the dural sac area significantly decreased on average by 5.2% (95%CI: 4.1%, 6.2%, *P* < 0.001; Table 3).

Intervertebral foramen

The area of the intervertebral foramina decreased on average by 3.4% (95%CI: 2.7%, 4.1%, *P* < 0.001) except for the L5-S1 section of the spine, which increased by 2.0% on average (95%CI: 0.5%, 3.9%, *P* = 0.045; Table 4).

Lumbosacral angle

The lumbosacral angles increased, on average, by 7.7% (95%CI: 5.7%, 9.6%, *P* < 0.001; Table 5).

Correlation analysis

A statistically significant correlation between exaggerated lumbosacral angle and age was found (Pearson correlation coefficient (*r*) = -0.253, *P* < 0.05). The negative correlation indicated that axial force on increasing lumbar lordosis in older patients is

Table 1 Three-dimensional Volume ISotropic Turbo spin-echo Acquisition magnetic resonance pulse parameters

Parameters	3D VISTA T2
Repetition time/Echo time (ms)	2000/90
Number of signal averaging	1
Field of View (mm)	300 × 200 × 75
Acquisition matrix	300 × 196
Acquisition voxel (mm)	1 × 1 × 0.5
Reconstruction matrix	640
Reconstruction voxel (mm)	0.47 × 0.47 × 0.5
Turbo factor	61
Sensitivity encoding factor	1.3
Scan time	06:46

3D: Three-dimensional; VISTA: Volume ISotropic Turbo spin-echo Acquisition.

Table 2 Cross-sectional area of the ligamentum flavum on the same levels with and without axial loading on both sides

Ligamenta flava(right + left) / section of the spine	Mean difference of area between unloaded and axial loading (%)	95%CI		*P* value
		Lower	Upper	
L1-L2	4.1	1.8	6.4	0.001
L2-L3	4.8	2.0	7.6	0.001
L3-L4	4.0	0.5	4.7	0.024
L4-L5	2.1	-0.5	6.3	0.116
L5-S1	4.1	2.5	5.2	< 0.001
All from L1-L2 to L5-S1	3.8	2.5	5.2	< 0.001

Negative value corresponds to a decrease. CI: Confidence interval.

less than in younger patients. Neither the area of the intervertebral foramina nor the area of the dural sac was correlated with age. Additionally, a percentage difference of the sagittal cross-section area of vertebral foramina, the cross-section area of the dural sac and ligamenta flava and the percentage difference of the lumbosacral angles did not significantly correlate with sex. The relationship testing between spine structure parameters did not deliver any significant association between any variables.

Degenerative changes
Degenerative changes of the lumbar spine are listed in Table 6.

DISCUSSION

Compression devices can be applied to high-field units. Therefore, high-resolution, 3D MRI might be obtained. This advantage of recumbent axially loaded MRI creates possibilities in determining the precise measurements and making an accurate diagnosis. The upright MRI would be a theoretically ideal diagnostic tool to simulate the spinal column under physiological conditions, but those systems are low-field MRI, which provides low image quality. Other studies have simultaneously analyzed several anatomical structures in the lumbar spine using upright, open and low-field (0.5T *vs* 1.5T in our study) MRI[33].

Table 3 Percentage difference of the cross-sectional area of the dural sac on transverse, T2-dependent magnetic resonance imaging at the same levels for phases both with and without axial loading

Dural sac/section of the spine	Mean difference of area between unloaded and axial loading (%)	95%CI		*P* value
		Lower	Upper	
L1-L2	-2.6	-3.6	-1.6	< 0.001
L2-L3	-5.5	-6.8	-4.2	< 0.001
L3-L4	-6.7	-8.9	-4.4	< 0.001
L4-L5	-8.1	-10.5	-5.7	< 0.001
L5-S1	-3.0	-4.9	-1.0	0.004
All from L1-L2 to L5-S1	-5.2	-6.2	-4.1	< 0.001

Negative values correspond to a decrease. CI: Confidence interval.

Table 4 Percentage difference of the sagittal cross-sectional area of vertebral foramina on the same levels both with and without axial loading on both sides

Intervertebral foramina (right + left)/section of the spine	Mean difference of area between unloaded and axial loading (%)	95%CI		*P* value
		Lower	Upper	
L1-L2	-4.0	-5.1	-2.9	< 0.001
L2-L3	-6.7	-8.0	-5.5	< 0.001
L3-L4	-5.1	-6.2	-4.0	< 0.001
L4-L5	-3.3	-4.8	-1.7	< 0.001
L5-S1	2.0	0.5	3.9	0.045
All from L1-L2 to L5-S1	-3.4	-4.1	-2.7	< 0.001

Negative values correspond to a decrease. CI: Confidence interval.

Table 5 Percentage difference of the lumbosacral angles between L1 and S1 measured based on recumbent and axial-loaded magnetic resonance images

Lumbosacral angle	Mean difference of angle between unloaded and axial loading (%)	95%CI		*P* value
		Lower	Upper	
From L1 to S1	7.7	5.7	9.6	< 0.001

CI: Confidence interval.

Contrary to our study, the previous study group was limited to young (*vs* any age in our study), less populated (12 *vs* 90 in our study) asymptomatic volunteers. No 3D high-resolution images and failure to measure several anatomical structures were reported. The proposed idea of applying axial-loaded MRI aimed to mimic as close as possible the load conditions occurring in the upright position. That position is currently impossible to apply in conventional recumbent high-field MRI. Devices intended for axial loading are commercially available and approved by the United States Food and Drug Administration. They also meet the New Approach Directive requirements of the European Union; yet, according to many authors, they are still in their experimental stage[43]. As a result, biomechanical testing has focused on many spinal structures simultaneously. The load distribution among the dural sac, ligamenta flava, intervertebral foramina and lumbar sagittal alignment was considered in this

Table 6 Degenerative pathologies of the lumbar spine

Analyzed factors	Grade	n	%
Intervertebral disc degeneration according to Pfirrmann *et al*[38] classification	1	0	0
	2	72	16
	3	196	44
	4	159	35
	5	23	5
Facet joint degeneration, according to Weishaupt *et al*[39] classification	0	300	33
	1	405	45
	2	149	17
	3	46	5
Grade of lumbar spinal canal stenosis according to Schizas *et al*[40] classification	A1	349	78
	A2	22	5
	A3	47	10
	A4	3	1
	B	20	4
	C	7	2
	D	2	0
Disc herniation according to the Michigan State University[42] classification of lumbar disc herniation	0	342	76
	1a, 1b, 1ab, 1c	88	20
	2a, 2b, 2ab, 2c	18	4
	3a, 3b, 3ab, 3c	2	0
Foraminal stenosis, according to Lee *et al*[41] classification	0	664	74
	1	168	19
	2	56	6
	3	12	1

spinal biomechanical assessment.

Dural sac

The dural sac occupies the most significant part of the spinal canal. Therefore, spinal stenosis mainly affects the dural sac, narrowed in the highest grade from all structures filling the spinal canal (Figure 2). The cross-sectional dural sac area measurement provides the most precise assessment of the spinal canal, but its time consumption is the main disadvantage of this method[44]. The results in this study showed that the mean dural sac cross-sectional area was significantly lower when loaded than relaxed at all lumbar spine levels from L1-L2 to L5-S1 (Figure 2). The rates of dynamic change were the highest at L4-L5 (mean of 8.1%; range of 5.7%-10.5%) and the lowest at L1-L2 (mean of 2.6%; range of 1.6%-3.6%).

The high sensitivity and specificity of axial-loaded MRI for detecting severe constriction were demonstrated by Kanno *et al*[32]. MRI examinations under axial loading are highly relevant in detecting central stenosis of the spinal canal, as to be confirmed by results reported by other authors[45]. Axial-loaded MRI demonstrated a significant reduction in the dural sac size and significant correlations of dural sac diameters with the upright myelogram. Therefore, axial-loaded MRI can be used to represent positional changes in dural sac size detected by upright myelography in patients with lumbar spinal canal stenosis[32]. Numerous *in vitro* experiments showed that axial loading results in spinal canal stenosis.

Schonstrom *et al*[25] specified that axial loading results in a spinal canal volume reduction in a spine segment, measured at an intervertebral disc level by about 40-50 mm^2. In their previous studies, the authors discovered that a pressure increase in the
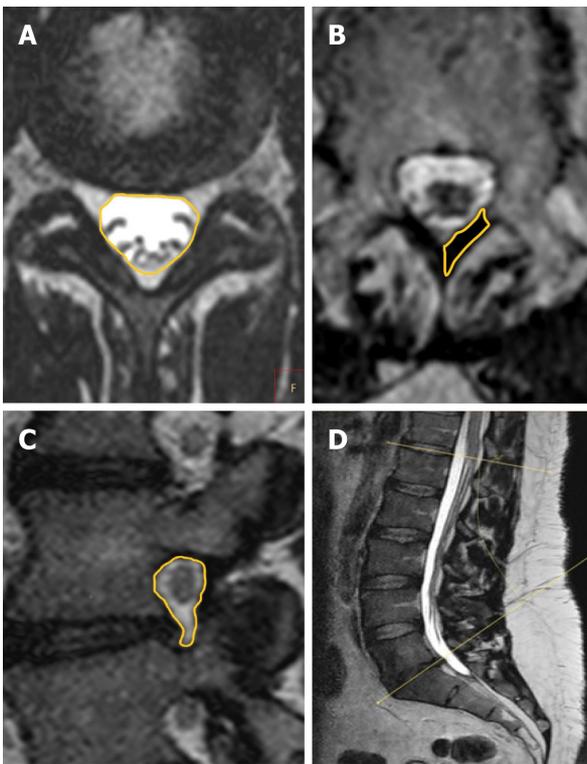
Figure 1 Specific measurements of (A) the cross-section area of the dural sac on transverse magnetic resonance imaging, (B) the cross-section area of the ligamentum flavum, (C) the sagittal cross-section area of vertebral foramina and (D) the lumbosacral angles between L1 and S1.
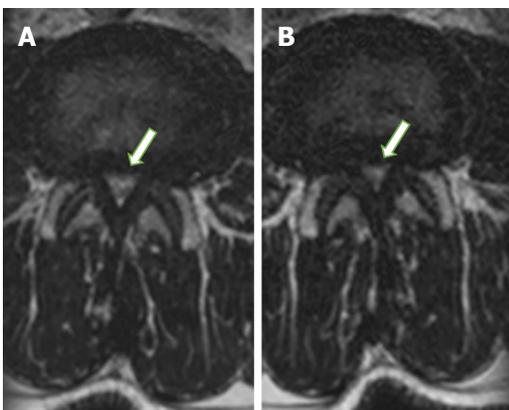
Figure 2 Transverse magnetic resonance imaging. A: Recumbent T2-weighted images. The rootlets occupy the whole of the dural sac (arrow), but they can still be individualized; B: Spinal stenosis with a reduction in the dural sac size after axial loading. No rootlets can be recognized, but some cerebrospinal fluid is still present, giving a grainy appearance to the sac (arrow).

dural sac of spinal segments reduces the spinal canal area down to approximately 79 mm^2[46]. Based on this discovery, contemporary authors assumed that 75 mm^2 is the borderline value of the dural sac cross-sectional area. Below this value, the authors suggested a diagnosis of absolute stenosis, and the range of 75-100 mm^2 indicates a diagnosis of relative spinal canal stenosis. Kim *et al*[47] arbitrarily defined a 10% reduction in the dural sac cross-sectional area as a significant reduction. They found a significant reduction in the cross-sectional area of the dural sac in 42% of patients, of which severe stenosis with a cross-sectional area lower than 75 mm^2 was found in 25% of patients.

Danielson and Willen[31] described an additional significant decrease in the cross-sectional area of the dural sac with axial-loading MRI as an area change more than 15 mm^2. They concluded that axial-loading MRI provided "additional, significant information" in 50 of 172 patients (29%). They also observed additional significant

findings in 69% of patients with neurogenic claudication, 14% of patients with sciatica and 0% of patients with LBP[31]. Of patients studied by Manenti *et al*[48], who were subjected to axial-loading MRI, 18 (45%) displayed cases of spinal canal stenosis emergence, 8 (20%) displayed cases of hernia enlargement, and 6 (15%) showed profound spondylolisthesis.

Ligamentum flavum

The ligamenta flava fills the space between the vertebral arches. They run just behind the facet joint and act as an extra reinforcement of the joint capsule. The ligamenta flava thickens with age. The ligamenta flava thickening is connected to fibrous tissue hypertrophy, which is a result of cyclooxygenase-2 and transforming growth factor-beta expression[49,50]. The changes are prominent in the dorsal part of the ligamenta flava, where the most potent axial load forces are observed[49]. This study showed that the mean cross-sectional area of the ligamenta flava was significantly higher when loaded than relaxed at all lumbar spine levels from L1-L2 to L5-S1. The rates of dynamic changes were the highest at L2-L3 (mean of 4.8%; range of 2.0%-7.6%) and the lowest at L4-L5.

According to the study of Hansson *et al*[45], it is not intervertebral discs but the ligamenta flava that have the most significant impact on spinal stenosis, being responsible for 50%-80% of spinal stenosis induced by axial loading. The case report of dynamic lumbar spinal stenosis with neurogenic claudication caused by the thickening of the ligamentum flavum, with MRI in decumbency, revealed no definite pathologic condition associated with symptoms[51]. According to some authors, the pathogenesis of thickening of the ligamentum flavum is unclear, and whether ligamentum flavum thickening is due to tissue hypertrophy or buckling remains controversial. Some studies claimed that canal narrowing, in part, results from the hypertrophy of the ligamentum flavum. In contrast, others argued that the ligamentum flavum bulges inside the spinal canal and compresses nerve tissues[49,50,52]. This information is relevant clinically because spinal stenosis may be underdiagnosed with regular MRI, and surgical intervention without adequate decompression may lead to poor outcomes.

Intervertebral foramen

Intervertebral foramina are triangular or oval at the lumbar level and broader in the coronal than the sagittal plane. Measurements recorded by encircling the intervertebral foramina sagittal cross-sections were proposed as the most accurate[53]. Our analysis of lumbar neural foramina showed that variation in the cross-sectional area of the neural foramen in the lumbar spine was significantly axially-loaded-dependent. We identified a statistically significant decrease in average percent foraminal area from recumbent to axially loaded at all levels except at L5-S1. Surprisingly, intervertebral foramina at L5-S1 widened after axial loading by 2%, on average (Figure 3).

Iwata *et al*[54] reported similar findings in computed tomography examinations using DynaWell equipment. They observed an enlargement of the intervertebral foramina area at the L5-S1 level and a simultaneous reduction in the intervertebral foramina area at L1-L2 levels to L4-L5 after axial loading. Conversely, MRI studies demonstrated a decrease in the foraminal area at all levels during weight-bearing in neutral, flexion and extension positions compared to unloaded supine imaging. The magnitude of change in the foraminal area increased as an angular motion at the segment increased. The most significant average percent decrease in the foraminal area occurs at L2-L3 and the smallest change at L5-S1, but a reduction at this level was still observed[53]. Therefore, changes caused by a compression device in foraminal dimensions at L5-S1 do not simulate physiological standing conditions.

Suppose the different types of loading simulated by DynaWell equipment and those occurring in the standing position responsible for differences in foraminal stenosis observed in those methods have not yet been determined. The axial load may be transmitted to the feet and the buttocks in the supine position. A reaction force acts on the buttocks causing the posterior rotation of the pelvis. That results in a significant decrease in the pelvic angle during axial loading[55]. According to Hioki *et al*[56], the disc wedge angles at the L5-S1 level with axial loading using DynaWell equipment differed from those in the standing posture. The magnitudes of changes were significantly smaller than in the standing position. They suggested that axial loading of the lumbar spine in the supine position decreases the angle between the L5 and S1 [56]. However, the L5-S1 angle did not significantly change in the standing posture than the controls in the supine position at rest. These observations of different lumbar-pelvic angular behavior could correspond with an enlargement of the area of intervertebral foramina at the L5-S1 level observed in our study. An awareness of these
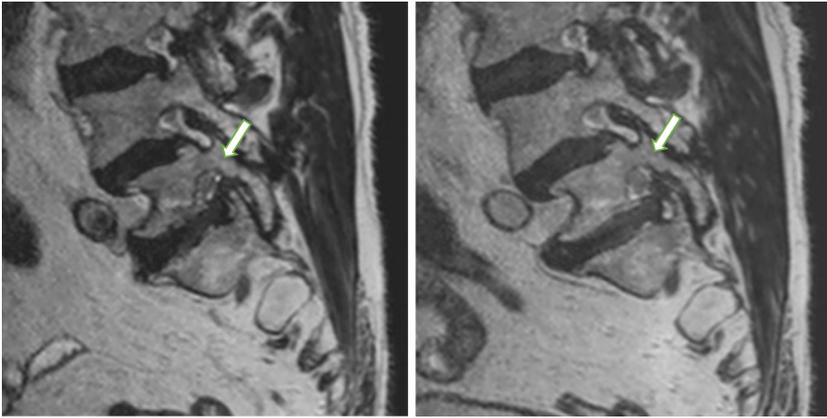
Figure 3 Sagittal magnetic resonance imaging. Morphologic changes in a foraminal zone at L5-S1 (arrow) with nerve root collapse and perineural fat obliteration were seen with and without axial loading.

phenomena is essential to allow clinicians to evaluate imaging results accurately.

The results in this study showed that the most significant foraminal constriction was by 6.7% (range of 5.5%-8.0%) under loading occurred at the L2-L3 level. Diagnostic benefits with a high grade of foraminal spinal detection could be achieved if inclusion criteria were limited to the suspicion of single spinal nerve involvement, as described by Splendiani *et al*[57]. They detected foraminal spinal stenosis at 61 of 230 levels and called it "hidden" stenosis, as it was not revealed on conventional recumbent MR examinations; it was only detected on examinations performed with the patient in the orthostatic position. The authors also discovered that stenosis of the intervertebral foramen was never found either in the presence of normal intervertebral discs or in the absence of facet disease in either the clinostatic or orthostatic position[57].

Lumbosacral angle
The spine is highly resistant to axial pressure. That resistance depends on the size and shape of the spine as well as spine curvatures. The human spine, at an early stage, consists of only one curvature: spine kyphosis. The following curvatures occur when the human develops the erected position: (1) At the cervical level: lordosis (cervical lordosis); (2) At the thoracic level: kyphosis (thoracic kyphosis); (3) At the lumbar level: lordosis (lumbar lordosis); and (4) At a sacral level: kyphosis (sacral kyphosis).

Curvatures in the sagittal plane make the spine more durable compared to the straight column. Therein one function of the lumbar lordosis is to provide a higher bearing resistance. Lumbar lordosis in the sagittal plane of the spine is unique only in the human population. It is not observed in any other animal. The changes in lordosis markedly affect the stabilizing sagittal moments.

Our results indicated that lordosis of the spine varies from the initial sagittal curvature by +7.7° after axial loading, responsible for more lordotic posture. Older patients show lower increases in lumbar lordosis when exposed to an axial force. As we observed a decreased elasticity of the spine in the older population, it is worth proposing axial-loading MRI as elasticity imaging: an innovative "elastography" method designed for the lumbar spine to explore the age of the spine, the percentile grids of degenerative changes.

Huang *et al*[58] reported that the mean lumbosacral angle was 37° in unloaded MRI examinations and increased to 39° after axial loading. Our lumbar spine biomechanics analysis also showed that axial loading increases lumbar lordosis. According to Hioki *et al*[56], lumbar axial loading with DynaWell in the supine position can simulate the lumbar spine position in the standing position. This loading device alters lumbar sagittal alignment differently from an upright standing position at the L5-S1 level.

Conversely, lumbar lordosis was more extensive after the axial load in the supine position compared to the standing position, according to Madsen *et al*[59]. This intriguing observation that the lumbosacral angle was 6° larger in the supine position than in the standing position, as explained by the author, was due to patients leaning against MRI walls to maintain a safe position and immobility when standing. Meakin *et al*[60] suggested that patients in the standing position are exposed to additional bearing forces. Patients with a lumbosacral angle smaller than the mean in an unloaded examination tend to straighten the spine after additional bearing forces. Patients with a lumbosacral angle greater than the mean in an unloaded examination

were observed to increase lumbar lordosis after additional bearing forces.

Correlation analysis

Simultaneous measurements of the percentage difference of the sagittal cross-section area of vertebral foramina, the cross-section areas of the dural sac and ligamenta flava as well as the percentage difference of the lumbosacral angles offered new information. According to our data, a statistically significant correlation exists between exaggerated lumbosacral angle and age (r = -0.253, $P < 0.05$). A negative correlation was found and showed that older patients have a lower increase in lumbar lordosis when exposed to axial force, similar to that found in the spine in the standing position. The percentage difference of the sagittal cross-section area of vertebral foramina, the cross-section areas of the dural sac and ligamenta flava, as well as the percentage difference of the lumbosacral angles, did not significantly correlate with each other and sex.

Limitations

This study has significant limitations. The research's main limitation is that all patients in the study were referred for MRI examinations for LBP, and there was no asymptomatic healthy control group. These results may not apply to asymptomatic, dynamic foraminal or spinal stenosis in the healthy population. Another potential limitation is that the inter-rater assessment has not been calculated. The force equal to half the body weight may not necessarily represent the lumbar spine load while standing. There may be a bias of data in the comparison between axial loading and standing conditions. Further comparative analyses between standing and axially-loaded MRI findings in the supine position would provide more clinically relevant information.

Another source of weakness in this study was the lack of computational approach in automatic image recognition based on machine learning and deep learning to ease radiological measurements of the lumbar spine. However, it is within the scope of our scientific interests, and we hope to expand artificial intelligence in image recognition and segmentation to automate lumbar spine assessment and to obtain a good level of clinical prediction. In our opinion, high resolution 3D imaging will make automatic image recognition more accurate. We showed in this study, that high resolution 3D MRI is feasible under axial compression. Volume ISotropic Turbo spin-echo Acquisition techniques have been used to acquire high-resolution, contiguous, thin-section isotropic images for complex spine anatomy and replace several two-dimensional acquisitions. The voxels generated by the 3D acquisition are submillimeter and measure the same in each direction, allowing the images to be reformatted with equal resolution in any direction.

CONCLUSION

The lumbar spine MRI is one of the most frequently performed examinations of all MRIs, but the MRI does not correlate significantly with back pain causes. The current study may help clinical practice understand spine physiology exposed to external forces, better-clarifying indications for axial load, and help identify the relationship between imaging examination results and perceived symptoms. A comparative evaluation of images obtained before and after axial loading of the spine showed changes in lumbosacral angles between L1 and S1, the dural sac cross-sectional area, the sagittal cross-sectional area of the intervertebral foramina and the cross-sectional area of the ligamentum flavum. Consistency in detecting central stenosis and ligamenta flava thickening between studies supports using an axial load of 50% body weight to simulate relaxed standing in the supine position. Changes in foraminal dimensions at L5-S1 do not affect physiological standing conditions. Axial loading intensifies the narrowing of the intervertebral foramina. Applying an axial compressive load increases lumbar lordosis, whereas the smallest changes were observed in older patients.

ARTICLE HIGHLIGHTS

Research background
Biomechanics of the individual lumbar spine structures are important since the overall spinal adaptation to compressive forces is comprised of the cumulative changes of respective elements.

Research motivation
There is a lack of works simultaneously comparing dural sac size, ligamenta flava thickness, foraminal dimensions and lumbar sagittal alignment between axial loaded and recumbent magnetic resonance imaging (MRI) in an extensive group of lower back pain patients.

Research objectives
To help the surgeons in the choice of the spinal endoscopy and spinal injections. The objective of the study was to evaluate the changes depicted by MRI of chosen lumbar spine structures upon axial-loading in comparison with recumbent MRI.

Research methods
The study covered 90 individuals assessed with three-dimensional volume isotropic acquisition MRI, first imaged in the supine position with no axial load and then again following application of an axial compressive load. Based on recumbent MRI as well as axial-loaded ones, the following were measured: the dural sac area, the ligamenta flava, the intervertebral foramina from L1-L2 to L5-S1 and the lumbosacral angle.

Research results
We found out that axial loading intensifies the narrowing of the spinal canal, thickens the ligamenta flava, narrows the intervertebral foramina from L1-L2 to L4-L5 and exaggerates lumbar lordosis.

Research conclusions
Our study reveals that there is a correlation between force compression and intensification of the lumbar spinal stenosis, intervertebral foramina narrowing, ligamenta flava thickening as well as increasing lumbar lordosis due to axial loading.

Research perspectives
There is a need to introduce computational approaches in automatic image recognition based on machine learning and deep learning to ease radiological measurements of the lumbar spine and obtain a good level of clinical prediction. Moreover, it is worth proposing axial-loading MRI as an elasticity imaging: an innovative "elastography" method designed for the lumbar spine to explore the age of the spine and the percentile grids of degenerative changes.

REFERENCES

1 **Clark S**, Horton R. Low back pain: a major global challenge. *Lancet* 2018; **391**: 2302 [PMID: 29573869 DOI: 10.1016/S0140-6736(18)30725-6]

2 **Croft PR**, Dunn KM, Raspe H. Course and prognosis of back pain in primary care: the epidemiological perspective. *Pain* 2006; **122**: 1-3 [PMID: 16530969 DOI: 10.1016/j.pain.2006.01.023]

3 **Dunn KM**, Croft PR. Epidemiology and natural history of low back pain. *Eura Medicophys* 2004; **40**: 9-13 [PMID: 16030488]

4 **Dunn KM**, Hestbaek L, Cassidy JD. Low back pain across the life course. *Best Pract Res Clin Rheumatol* 2013; **27**: 591-600 [PMID: 24315141 DOI: 10.1016/j.berh.2013.09.007]

5 **van der Windt DA**, Dunn KM. Low back pain research--future directions. *Best Pract Res Clin Rheumatol* 2013; **27**: 699-708 [PMID: 24315150 DOI: 10.1016/j.berh.2013.11.001]

6 **Gore M**, Sadosky A, Stacey BR, Tai KS, Leslie D. The burden of chronic low back pain: clinical comorbidities, treatment patterns, and health care costs in usual care settings. *Spine* 2012; **37**: E668-E677 [PMID: 22146287 DOI: 10.1097/BRS.0b013e318241e5de]

7 **Balagué F**, Mannion AF, Pellisé F, Cedraschi C. Non-specific low back pain. *Lancet* 2012; **379**: 482-491 [PMID: 21982256 DOI: 10.1016/S0140-6736(11)60610-7]

8 **Stewart WF**, Ricci JA, Chee E, Morganstein D, Lipton R. Lost productive time and cost due to common pain conditions in the US workforce. *JAMA* 2003; **290**: 2443-2454 [PMID: 14612481 DOI:

10.1001/jama.290.18.2443]

9   **Freburger JK**, Holmes GM, Agans RP, Jackman AM, Darter JD, Wallace AS, Castel LD, Kalsbeek WD, Carey TS. The rising prevalence of chronic low back pain. *Arch Intern Med* 2009; **169**: 251-258 [PMID: 19204216 DOI: 10.1001/archinternmed.2008.543]

10   **Burton AK**, Balagué F, Cardon G, Eriksen HR, Henrotin Y, Lahad A, Leclerc A, Müller G, van der Beek AJ; COST B13 Working Group on Guidelines for Prevention in Low Back Pain. Chapter 2. European guidelines for prevention in low back pain : November 2004. *Eur Spine J* 2006; **15** Suppl 2: S136-S168 [PMID: 16550446 DOI: 10.1007/s00586-006-1070-3]

11   **Meucci RD**, Fassa AG, Faria NM. Prevalence of chronic low back pain: systematic review. *Rev Saude Publica* 2015; **49** [PMID: 26487293 DOI: 10.1590/S0034-8910.2015049005874]

12   **GBD 2017 Disease and Injury Incidence and Prevalence Collaborators**. Global, regional, and national incidence, prevalence, and years lived with disability for 354 diseases and injuries for 195 countries and territories, 1990-2017: a systematic analysis for the Global Burden of Disease Study 2017. *Lancet* 2018; **392**: 1789-1858 [PMID: 30496104 DOI: 10.1016/S0140-6736(18)32279-7]

13   **Hurwitz EL**, Randhawa K, Yu H, Côté P, Haldeman S. The Global Spine Care Initiative: a summary of the global burden of low back and neck pain studies. *Eur Spine J* 2018; **27**: 796-801 [PMID: 29480409 DOI: 10.1007/s00586-017-5432-9]

14   **Bogduk N**. Functional anatomy of the spine. *Handb Clin Neurol* 2016; **136**: 675-688 [PMID: 27430435 DOI: 10.1016/B978-0-444-53486-6.00032-6]

15   **Izzo R**, Popolizio T, D'Aprile P, Muto M. Spinal pain. *Eur J Radiol* 2015; **84**: 746-756 [PMID: 25824642 DOI: 10.1016/j.ejrad.2015.01.018]

16   **Kinder A**, Filho FP, Ribeiro E, Domingues RC, Marchiori E, Gasparetto E. Magnetic resonance imaging of the lumbar spine with axial loading: a review of 120 cases. *Eur J Radiol* 2012; **81**: e561-e564 [PMID: 21741192 DOI: 10.1016/j.ejrad.2011.06.027]

17   **Lorme KJ**, Naqvi SA. Comparative analysis of low-back loading on chiropractors using various workstation table heights and performing various tasks. *J Manipulative Physiol Ther* 2003; **26**: 25-33 [PMID: 12532135 DOI: 10.1067/mmt.2003.43]

18   **Granata KP**, Marras WS. Relation between spinal load factors and the high-risk probability of occupational low-back disorder. *Ergonomics* 1999; **42**: 1187-1199 [PMID: 10503053 DOI: 10.1080/001401399185072]

19   **Han JS**, Goel VK, Ahn JY, Winterbottom J, McGowan D, Weinstein J, Cook T. Loads in the spinal structures during lifting: development of a three-dimensional comprehensive biomechanical model. *Eur Spine J* 1995; **4**: 153-168 [PMID: 7552650 DOI: 10.1007/BF00298240]

20   **Nachemson A**. The load on lumbar disks in different positions of the body. *Clin Orthop Relat Res* 1966; **45**: 107-122 [PMID: 5937361]

21   **Nachemson A**, Elfström G. Intravital dynamic pressure measurements in lumbar discs. A study of common movements, maneuvers and exercises. *Scand J Rehabil Med Suppl* 1970; **1**: 1-40 [PMID: 4257209]

22   **Nachemson AL**. Disc pressure measurements. *Spine* 1981; **6**: 93-97 [PMID: 7209680 DOI: 10.1097/00007632-198101000-00020]

23   **Rohlmann A**, Graichen F, Bender A, Kayser R, Bergmann G. Loads on a telemeterized vertebral body replacement measured in three patients within the first postoperative month. *Clin Biomech (Bristol, Avon)* 2008; **23**: 147-158 [PMID: 17983694 DOI: 10.1016/j.clinbiomech.2007.09.011]

24   **Rohlmann A**, Petersen R, Schwachmeyer V, Graichen F, Bergmann G. Spinal loads during position changes. *Clin Biomech (Bristol, Avon)* 2012; **27**: 754-758 [PMID: 22571842 DOI: 10.1016/j.clinbiomech.2012.04.006]

25   **Schönström N**, Lindahl S, Willén J, Hansson T. Dynamic changes in the dimensions of the lumbar spinal canal: an experimental study in vitro. *J Orthop Res* 1989; **7**: 115-121 [PMID: 2908901 DOI: 10.1002/jor.1100070116]

26   **Koes BW**, van Tulder M, Lin CW, Macedo LG, McAuley J, Maher C. An updated overview of clinical guidelines for the management of non-specific low back pain in primary care. *Eur Spine J* 2010; **19**: 2075-2094 [PMID: 20602122 DOI: 10.1007/s00586-010-1502-y]

27   **Maher C**, Underwood M, Buchbinder R. Non-specific low back pain. *Lancet* 2017; **389**: 736-747 [PMID: 27745712 DOI: 10.1016/S0140-6736(16)30970-9]

28   **Sasani H**, Solmaz B, Sasani M, Vural M, Ozer AF. Diagnostic Importance of Axial Loaded Magnetic Resonance Imaging in Patients with Suspected Lumbar Spinal Canal Stenosis. *World Neurosurg* 2019; **127**: e69-e75 [PMID: 30857995 DOI: 10.1016/j.wneu.2019.02.091]

29   **Lorenc T**, Palczewski P, Wójcik D, Glinkowski W, Gołębiowski M. Diagnostic Benefits of Axial-Loaded Magnetic Resonance Imaging Over Recumbent Magnetic Resonance Imaging in Obese Lower Back Pain Patients. *Spine* 2018; **43**: 1146-1153 [PMID: 30059481 DOI: 10.1097/BRS.0000000000002532]

30   **Maquer G**, Brandejsky V, Benneker LM, Watanabe A, Vermathen P, Zysset PK. Human intervertebral disc stiffness correlates better with the Otsu threshold computed from axial T2 map of its posterior annulus fibrosus than with clinical classifications. *Med Eng Phys* 2014; **36**: 219-225 [PMID: 24309128 DOI: 10.1016/j.medengphy.2013.11.008]

31   **Danielson BI**, Willén J, Gaulitz A, Niklason T, Hansson TH. Axial loading of the spine during CT and MR in patients with suspected lumbar spinal stenosis. *Acta Radiol* 1998; **39**: 604-611 [PMID: 9817029 DOI: 10.3109/02841859809175484]

32   **Kanno H**, Endo T, Ozawa H, Koizumi Y, Morozumi N, Itoi E, Ishii Y. Axial loading during

magnetic resonance imaging in patients with lumbar spinal canal stenosis: does it reproduce the positional change of the dural sac detected by upright myelography? *Spine* 2012; **37**: E985-E992 [PMID: 21258271 DOI: 10.1097/BRS.0b013e31821038f2]

33 **Schmid M**, Stucki G. , Duewell S. Changes in cross-sectional measurements of the spinal canal and intervertebral foramina as a function of body position: in vivo studies on an open-configuration MR system. *AJR Am J Roentgenol* 1999; **172**: 1095-1102 [PMID: 10587155 DOI: 10.2214/ajr.172.4.10587155]

34 **Lewandrowski KU**. Retrospective analysis of accuracy and positive predictive value of preoperative lumbar MRI grading after successful outcome following outpatient endoscopic decompression for lumbar foraminal and lateral recess stenosis. *Clin Neurol Neurosurg* 2019; **179**: 74-80 [PMID: 30870712 DOI: 10.1016/j.clineuro.2019.02.019]

35 **Sairyo K**, Chikawa T, Nagamachi A. State-of-the-art transforaminal percutaneous endoscopic lumbar surgery under local anesthesia: Discectomy, foraminoplasty, and ventral facetectomy. *J Orthop Sci* 2018; **23**: 229-236 [PMID: 29248305 DOI: 10.1016/j.jos.2017.10.015]

36 **Wagner R**, Haefner M. Indications and Contraindications of Full-Endoscopic Interlaminar Lumbar Decompression. *World Neurosurg* 2021; **145**: 657-662 [PMID: 32810629 DOI: 10.1016/j.wneu.2020.08.042]

37 **Park CH**, Lee SH. Endoscope-Assisted Minimally Invasive Interlaminar Lumbar Decompression for Spinal Stenosis. *Pain Physician* 2019; **22**: E573-E578 [PMID: 31775410]

38 **Pfirrmann CW**, Metzdorf A, Zanetti M, Hodler J, Boos N. Magnetic resonance classification of lumbar intervertebral disc degeneration. *Spine* 2001; **26**: 1873-1878 [PMID: 11568697 DOI: 10.1097/00007632-200109010-00011]

39 **Weishaupt D**, Zanetti M, Boos N, Hodler J. MR imaging and CT in osteoarthritis of the lumbar facet joints. *Skeletal Radiol* 1999; **28**: 215-219 [PMID: 10384992 DOI: 10.1007/s002560050503]

40 **Schizas C**, Theumann N, Burn A, Tansey R, Wardlaw D, Smith FW, Kulik G. Qualitative grading of severity of lumbar spinal stenosis based on the morphology of the dural sac on magnetic resonance images. *Spine* 2010; **35**: 1919-1924 [PMID: 20671589 DOI: 10.1097/BRS.0b013e3181d359bd]

41 **Lee S**, Lee JW, Yeom JS, Kim KJ, Kim HJ, Chung SK, Kang HS. A practical MRI grading system for lumbar foraminal stenosis. *AJR Am J Roentgenol* 2010; **194**: 1095-1098 [PMID: 20308517 DOI: 10.2214/AJR.09.2772]

42 **Mysliwiec LW**, Cholewicki J, Winkelpleck MD, Eis GP. MSU classification for herniated lumbar discs on MRI: toward developing objective criteria for surgical selection. *Eur Spine J* 2010; **19**: 1087-1093 [PMID: 20084410 DOI: 10.1007/s00586-009-1274-4]

43 **Dahabreh IJ**, Hadar N, Chung M. Emerging magnetic resonance imaging technologies for musculoskeletal imaging under loading stress: scope of the literature. *Ann Intern Med* 2011; **155**: 616-624 [PMID: 22041950 DOI: 10.7326/0003-4819-155-9-201111010-00009]

44 **Schonstrom NS**, Bolender NF, Spengler DM. The pathomorphology of spinal stenosis as seen on CT scans of the lumbar spine. *Spine* 1985; **10**: 806-811 [PMID: 4089655 DOI: 10.1097/00007632-198511000-00005]

45 **Hansson T**, Suzuki N, Hebelka H, Gaulitz A. The narrowing of the lumbar spinal canal during loaded MRI: the effects of the disc and ligamentum flavum. *Eur Spine J* 2009; **18**: 679-686 [PMID: 19277726 DOI: 10.1007/s00586-009-0919-7]

46 **Schönström N**, Bolender NF, Spengler DM, Hansson TH. Pressure changes within the cauda equina following constriction of the dural sac. An in vitro experimental study. *Spine* 1984; **9**: 604-607 [PMID: 6495030 DOI: 10.1097/00007632-198409000-00011]

47 **Kim YK**, Lee JW, Kim HJ, Yeom JS, Kang HS. Diagnostic advancement of axial loaded lumbar spine MRI in patients with clinically suspected central spinal canal stenosis. *Spine* 2013; **38**: E1342-E1347 [PMID: 23797506 DOI: 10.1097/BRS.0b013e3182a0dfa5]

48 **Manenti G**, Liccardo G, Sergiacomi G, Ferrante L, D'Andrea G, Konda D, Fraioli B, Schillaci O, Simonetti G, Masala S. Axial loading MRI of the lumbar spine. *In Vivo* 2003; **17**: 413-420 [PMID: 14598603]

49 **Sairyo K**, Biyani A, Goel V, Leaman D, Booth R Jr, Thomas J, Gehling D, Vishnubhotla L, Long R, Ebraheim N. Pathomechanism of ligamentum flavum hypertrophy: a multidisciplinary investigation based on clinical, biomechanical, histologic, and biologic assessments. *Spine* 2005; **30**: 2649-2656 [DOI: 10.1097/01.brs.0000188117.77657.ee]

50 **Sairyo K**, Biyani A, Goel VK, Leaman DW, Booth R, Jr. , Thomas J, Ebraheim NA, Cowgill IA, Mohan SE. Lumbar ligamentum flavum hypertrophy is due to accumulation of inflammation-related scar tissue. *Spine* 2007; **32**: E340-347 [DOI: 10.1097/01.brs.0000263407.25009.6e]

51 **Choi KC**, Kim JS, Jung B, Lee SH. Dynamic lumbar spinal stenosis : the usefulness of axial loaded MRI in preoperative evaluation. *J Korean Neurosurg Soc* 2009; **46**: 265-268 [PMID: 19844630 DOI: 10.3340/jkns.2009.46.3.265]

52 **Altinkaya N**, Yildirim T, Demir S, Alkan O, Sarica FB. Factors associated with the thickness of the ligamentum flavum: is ligamentum flavum thickening due to hypertrophy or buckling? *Spine* 2011; **36**: E1093-E1097 [PMID: 21343862 DOI: 10.1097/BRS.0b013e318203e2b5]

53 **Singh V**, Montgomery SR, Aghdasi B, Inoue H, Wang JC, Daubs MD. Factors affecting dynamic foraminal stenosis in the lumbar spine. *Spine J* 2013; **13**: 1080-1087 [PMID: 23669126 DOI: 10.1016/j.spinee.2013.03.041]

54 **Iwata T**, Miyamoto K, Hioki A, Ohashi M, Inoue N, Shimizu K. In vivo measurement of lumbar foramen during axial loading using a compression device and computed tomography. *J Spinal Disord*

Tech 2013; **26**: E177-E182 [PMID: 23381186 DOI: 10.1097/BSD.0b013e318286f635]

55   **Hioki A**, Miyamoto K, Shimizu K, Inoue N. Test-retest repeatability of lumbar sagittal alignment and disc height measurements with or without axial loading: a computed tomography study. *J Spinal Disord Tech* 2011; **24**: 93-98 [PMID: 21430497 DOI: 10.1097/BSD.0b013e3181dd611f]

56   **Hioki A**, Miyamoto K, Sakai H, Shimizu K. Lumbar axial loading device alters lumbar sagittal alignment differently from upright standing position: a computed tomography study. *Spine* 2010; **35**: 995-1001 [PMID: 20139804 DOI: 10.1097/BRS.0b013e3181bb8188]

57   **Splendiani A**, Ferrari F, Barile A, Masciocchi C, Gallucci M. Occult neural foraminal stenosis caused by association between disc degeneration and facet joint osteoarthritis: demonstration with dedicated upright MRI system. *Radiol Med* 2014; **119**: 164-174 [PMID: 24337755 DOI: 10.1007/s11547-013-0330-7]

58   **Huang KY**, Lin RM, Lee YL, Li JD. Factors affecting disability and physical function in degenerative lumbar spondylolisthesis of L4-5: evaluation with axially loaded MRI. *Eur Spine J* 2009; **18**: 1851-1857 [PMID: 19526378 DOI: 10.1007/s00586-009-1059-9]

59   **Madsen R**, Jensen TS, Pope M, Sørensen JS, Bendix T. The effect of body position and axial load on spinal canal morphology: an MRI study of central spinal stenosis. *Spine* 2008; **33**: 61-67 [PMID: 18165750 DOI: 10.1097/BRS.0b013e31815e395f]

60   **Meakin JR**, Smith FW, Gilbert FJ, Aspden RM. The effect of axial load on the sagittal plane curvature of the upright human spine in vivo. *J Biomech* 2008; **41**: 2850-2854 [PMID: 18715567 DOI: 10.1016/j.jbiomech.2008.06.035]